Optical-absorption profile of a single modulation-doped $Al_xGa_{1-x}As/GaAs$ heterojunction

E. S. Snow, O. J. Glembocki, and B. V. Shanabrook
Naval Research Laboratory, Washington, D.C. 20375-5000
(Received 23 May 1988; revised manuscript received 1 August 1988)

The interband optical properties of a single modulation-doped $Al_xGa_{1-x}As/GaAs$ heterojunction are calculated. The calculation includes the absorption from the extended valence-band states into the first five conduction-subband states which are confined by the band offset at the heterojunction and the space-charge potential. Modulation of the absorption is calculated under the assumption that the modulation mechanism is the variation of the two-dimensional electron concentration. The predominant effect of the modulation on the absorption arises from the modulation of the Burstein-Moss edge in the bottom subband. Results of the calculation are compared to experimental electroreflectance data and are found to be in agreement.

Modulation spectroscopy has gained popularity as a tool for studying and characterizing microstructures. Photoreflectance (PR) measurements provide a room-temperature contactless method for obtaining information such as alloy concentration and quantum-well width.[1-4] Both the modulation mechanisms and line shapes observed in PR measurements on quantum-well structures are reasonably well understood.[5,6] Recently, PR spectra of modulation-doped field-effect transistors (MODFET's) were shown to exhibit a feature which correlates with the presence of a two-dimensional electron gas (2D EG).[1,2] This work opens the possibility that PR might also provide a simple, room-temperature, contactless method for characterizing MODFET's. Subsequently, Yinsheng and Desheng also reported PR spectra of MODFET's.[7] A model describing the data was proposed which attributed the PR spectra to interband transitions from the valence band to the two-dimensional conduction subbands. The data were fit to the Aspnes's theory of modulation spectroscopy.[8] However, no modifications to the theory were made to take into account the distinguishing properties of a heterojunction, i.e., transitions involving 3D valence-band states and 2D conduction subbands in a high electric field.

Electroreflectance (ER) measurements of MODFET's have also been reported.[9] The feasibility of using ER effects for optical readout of transistor action was discussed. The electroreflectance results were explained in terms of modulation of the band-edge absorption due to Franz-Keldysh effects involving the quantum-confined states at the heterojunction. No calculation of the absorption process was presented.

In addition to the modulation experiments, several groups have reported photoluminescence features related to the $Al_xGa_{1-x}As/GaAs$ heterojunction.[10-13] Photoluminescence has been observed in samples both with 2D EG's and with 2D-hole gases.

In spite of these experimental efforts, few calculations of the interband optical properties of a single modulation-doped heterojunction have been reported. Duke[14] has examined the optical properties of a general semiconductor-oxide interface, although the subject of interband transitions was discussed only briefly.

In this paper, we calculate the interband absorption properties of a $GaAs/Al_xGa_{1-x}As$ modulation-doped heterojunction. The absorption is calculated between the extended states of the valence band and the quantum-confined states of the conduction band. The absorption process is analogous to the Franz-Keldysh effect with the modification that the states in the conduction band are not extended but are confined by the band offset and space-charge potential at the heterojunction.

Specific attention is paid to the modulation of the absorption resulting from changes in the 2D EG density. Surprisingly, the results of the calculation indicate no structure corresponding to the onset of absorption by the individual subbands. The only structure that is evident arises from Franz-Keldysh-like oscillations arising from structure in the energy dependence of the interband matrix elements between the conduction-subband and valence-band envelope functions.

For comparison, low-temperature experimental ER data are also presented. The line shape of the predominant feature in the ER spectra is in qualitative agreement with the calculation.

A schematic of the absorption process is shown in Fig. 1. The optical-absorption coefficient α between the valence band and the two-dimensional conduction subbands is given by

$$\alpha \propto \frac{1}{\hbar\omega}\sum_s \alpha_s = \frac{1}{\hbar\omega}\sum_{s,v}\alpha_{sv} ,$$

where the summation is taken over the valence-band (v) and conduction-subband (s) states. α_{sv} is given by

$$\alpha_{sv} = \sum_{k_\parallel} |\langle v|s\rangle|^2 \, |\hat{\varepsilon}\cdot\mathbf{p}|^2 \, \delta(E_s(k_\parallel) - E_v(k_\parallel) - \hbar\omega) ,$$

where $k_\parallel$ is the component of the wave vector parallel to the surface and the summation is taken over the unoccupied conduction-subband states, i.e., $E_s > E_F$, $\mathbf{p}$ is the matrix element of the momentum operator with the Bloch states of the crystal (assumed to be independent of k), and $\hat{\varepsilon}$ is the polarization vector of the incident light. $\langle v|s\rangle$ is

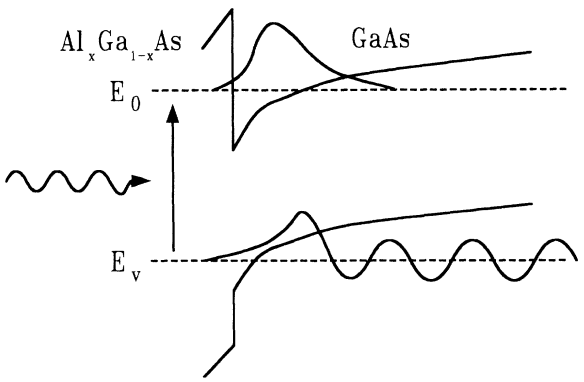

FIG. 1. Diagram of the band structure and the valence- and conduction-band states at the heterojunction. The potential and the bottom conduction subband are calculated using a self-consistent Hartree approximation. Next, the excited subbands and the valence-band states are calculated from the potential.

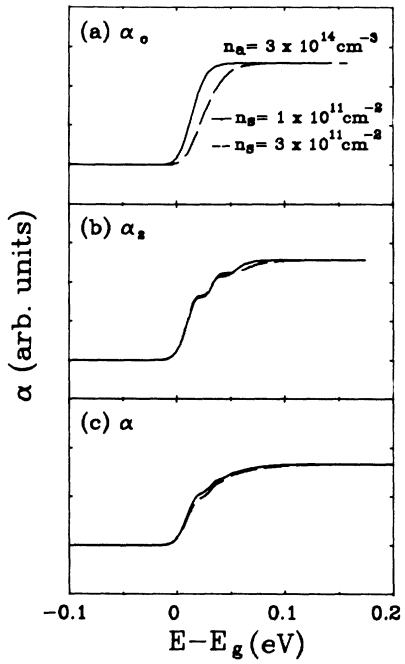

FIG. 2. Absorption vs energy plotted for two values of n_s and $n_a = 3\times10^{14}$ cm^{-3}. (a) and (b) represent the absorption into the bottom and second excited subbands. (c) represents the total absorption.

the overlap integral of the valence-band and conduction-subband envelope functions. The envelope functions $|s\rangle$ and $|v\rangle$ were calculated as follows. For a given value of the acceptor doping level in the GaAs and the 2D EG density n_s, the envelope function of the bottom subband and the potential were computed with a self-consistent Hartree approximation.[15,16] The conduction-band offset was taken to be 0.3 eV. From the potential, the higher subbands and the valence-band wave functions were numerically computed. A total of five conduction subbands were used in the calculation. The interband absorption was calculated from the summation of the appropriate overlap integrals of the envelope functions. Zero temperature was assumed throughout. Many-body effects were not included in the calculation due to the difficulty in properly calculating the energy shift and the wave functions of the valence-band states.

In Fig. 2(a), the absorption into the bottom subband is shown for two values of n_s with $n_a = 3\times10^{14}$ cm^{-3}. The energy width of the absorption edge for both densities is broad ($\sim$50 meV). The origin of the broadening is easily seen in Fig. 1. The subband envelope function extends well away from the $Al_xGa_{1-x}As/GaAs$ heterojunction. Over this region of the sample there is a large potential drop (of order E_0) due to the space charge n_s. Thus, a broad energy range of valence-band states will contribute to the overlap integrals with the subband state, resulting in a broad absorption edge.

As n_s is increased, the absorption edge broadens slightly and shifts to higher energy. The energy shift is due to the increase in the Fermi energy within the bottom conduction subband, analogous to the Burstein-Moss shift in a bulk semiconductor. Since the higher-lying subbands are not occupied at these densities, they do not experience this effect.

In Fig. 2(b) the absorption into the second excited subband is shown. The absorption edge is again broad and only a slight additional broadening results from an increase in n_s. The structure in the absorption edge is due to the energy dependence of $\langle v|s\rangle$. This energy dependence arises from interference between the oscillations of the valence-band envelope functions and the three lobes of the second excited subband.

Note that the absorption edge onset is at, or slightly below, the band-gap energy and not at E_g+E_s. The conduction-subband envelope functions extend out from the heterojunction to approximately the point where the subband energy levels cross the conduction band. At this point, the energy difference between the subband and the valence band is equal to the band-gap energy. Thus, the onset of absorption occurs at $\sim E_g$ instead of E_g+E_s.

The total absorption, including the first five subbands, is plotted in Fig. 2(c). Since the onset of the absorption for all the subbands is at approximately the band-gap energy (except for the first due to the position of the Fermi energy) there is no structure in the absorption edge that can be identified with the subband energies. This is an important observation since it implies that interband absorption is not a sensitive measurement of the energy positions of the subbands. The only structure evident in the absorption edge arises from oscillations in $\langle v|s\rangle$. It is unclear whether or not this structure will remain after absorption into the higher-energy subbands ($>E_4$) is included. The main effect of increasing n_s is the shift of the absorption edge of the bottom subband due to the increase in the Fermi energy. The slight broadening of the remaining subbands also alters the absorption slightly.

To simulate modulation spectroscopy, we calculate the change in absorption $\Delta\alpha$ as n_s is modulated. The modulated intensity of the reflected light in a PR or ER experiment is proportional to the superposition of the modulation of the real $\Delta\epsilon_1$ and imaginary $\Delta\epsilon_2$ parts of the dielec-

tric function. These two quantities were calculated from $\Delta\alpha$ using the Kronig-Kramers relations.

In Fig. 3, $\Delta\epsilon_1$ and $\Delta\epsilon_2$ are plotted for two values of n_s. The magnitude of the modulation was $\Delta n_s = 1\times10^{11}$ cm^{-2}. Since the dominate modulation mechanism is the Fermi-energy shift in the bottom subband, $\Delta\epsilon_2$ approximates the first derivative of α_0 with respect to E. Energy broadening of the excited subbands contributes additionally to $\Delta\epsilon_1$ and $\Delta\epsilon_2$. The structure in the high-energy tail of $\Delta\epsilon_1$ and $\Delta\epsilon_2$ is due to oscillations in $\langle v|s\rangle$ involving the excited subbands. As n_s is increased, $\Delta\epsilon_1$ and $\Delta\epsilon_2$ broaden and shift away from the band-gap energy corresponding to the analogous behavior of α_0.

Experimental ER data are shown in the top half of Fig. 4. The structure consisted of a 100-Å GaAs cap layer, a 400-Å Si-doped $Al_xGa_{1-x}As$ layer ($N_D = 2\times10^{18}$ cm^{-3}), a 100-Å $Al_xGa_{1-x}As$ spacer layer, and a 1-μm GaAs buffer layer grown on a semi-insulating GaAs substrate. The sample had a carrier concentration of 6×10^{11} cm^{-2} and a mobility of 97 000 cm^2/V s at 77 K. Contact to the 2D EG channel was made with diffused Au-Ge contacts. A semitransparent gate was evaporated onto the sample following the removal of the cap layer. The gate consisted of 10 Å of Cr followed by 60 Å of Au. The modulation spectra were produced by placing a 0.1-V modulation on a dc gate voltage. The spectra were taken at 10 K and are shown for two dc values of the gate voltage. The carrier concentrations quoted in Fig. 4 are estimates based on Hall-effect measurements on an ungated device.

Also shown in Fig. 4 are two calculations of the ER spectra. The spectra were produced by calculating the proper linear combination of $\Delta\epsilon_1$ and $\Delta\epsilon_2$ appropriate for this particular structure, as determined by the phase shifts of the light introduced at the reflections off the air-gate, gate-$Al_xGa_{1-x}As$, and $Al_xGa_{1-x}As$-GaAs boundaries.[17]

The experimental and theoretical curves are in qualitative agreement. However, there are three distinct differences. The first difference is the sharp structure at the band-gap energy which is present in the experimental data. This structure corresponds to absorption modulation of the bulk GaAs exciton. This absorption is not present in the calculation since we are only calculating the absorption in the high-field region of the heterojunction. The second difference is the structure present in the high-energy tail of the calculated data. As was mentioned above, it is unclear whether or not this structure would remain if absorption into the higher subbands is included. Alternatively, if the structure is real, the inhomogeneities introduced during the device fabrication may have sufficiently broadened the experimental data as to render the structure unobservable. The third difference is the energy shift between the experimental and calculated data. This energy difference most likely arises as the result of neglecting many-body corrections in the calculation. We have applied the local-density-functional approximation[16] to the calculation of the conduction subbands and find approximately a 5–10-meV downward shift in energy for these densities. If the valence-band states are similarly affected, the calculation would overestimate the absorption energy by approximately 10–20 meV. This energy shift accounts for the difference in energy between the calculation and the experimental data.

The PR data published in Refs. 1, 2, and 7 differ markedly from the present results. The experimental data indicate that the 2D EG PR feature is much narrower than the calculation predicts. More-recent PR

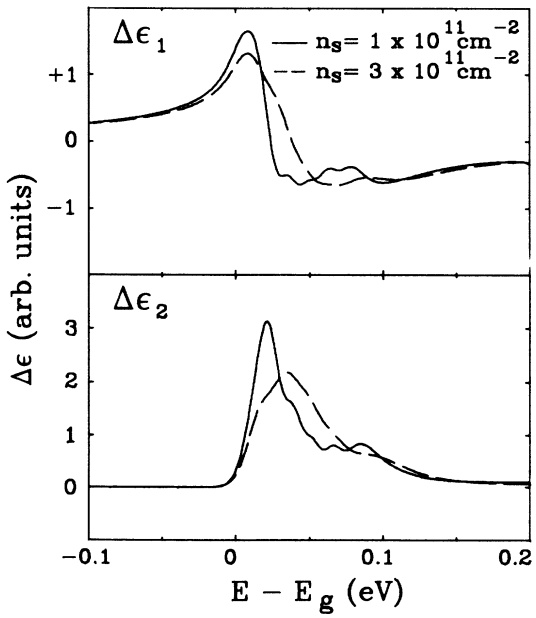

FIG. 3. The modulated real ($\Delta\epsilon_1$) and imaginary ($\Delta\epsilon_2$) parts of the dielectric function. The absorption was modulated by the variation of n_s, $\Delta n_s = 1\times10^{11}$ cm^{-2}.

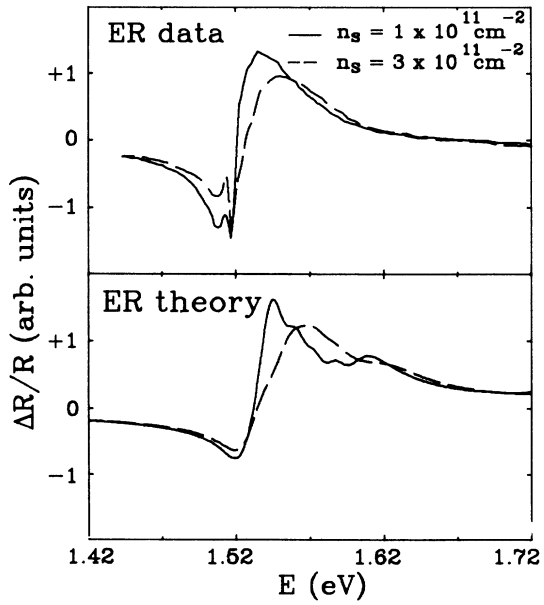

FIG. 4. Experimental ER data taken at 10 K. Reflections off the air-metal, metal-$Al_xGa_{1-x}As$, and $Al_xGa_{1-x}As$-GaAs interfaces mix $\Delta\epsilon_1$ and $\Delta\epsilon_2$. Calculation of the modulated reflected intensity is also shown. The experimental data and the calculation are in qualitative agreement.

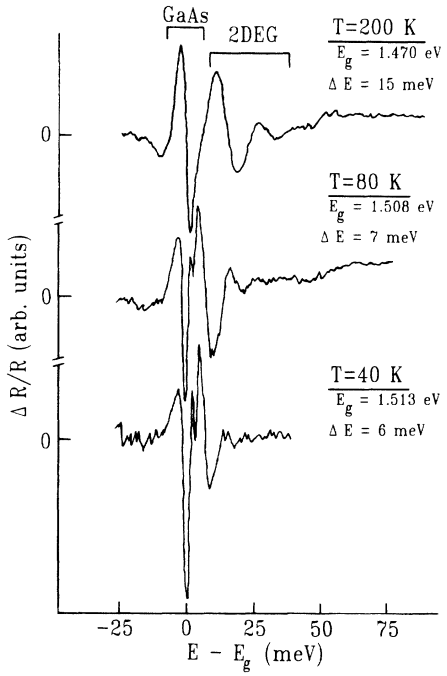

FIG. 5. PR data taken at 200, 80, and 40 K. In contrast to the ER data, the 2D EG PR feature is very narrow in energy ($\sim$6 meV).

data indicate that the 2D EG feature is only $\sim$6 meV wide at low temperature (see Fig. 5). This is to be compared with the $\sim$50 meV width of the ER feature shown in Fig. 4. Clearly, interband absorption, alone (as proposed in Ref. 7), cannot explain the PR results.

In PR, the operative modulation mechanism is the photogeneration of electron-hole pairs and their subsequent spatial redistribution. In the case of a MODFET, the photogenerated charge is produced predominantly in the GaAs buffer layer. The photogenerated electrons and holes both modulate n_s and flatten the energy bands across the depletion layer of the GaAs. The latter of the two effects is not modeled by the calculation in which n_s originates solely from the doped $Al_xGa_{1-x}As$ layer.[18] However, it is doubtful that sharp features will arise in $\Delta\epsilon_1$ or $\Delta\epsilon_2$ from modulation of the fields in the GaAs depletion region since α itself is broad. Possibly, the addition of impurity states or the inclusion of excitonic effects can explain the PR data.[19]

In summary, we have calculated the interband optical-absorption properties of a modulation-doped $Al_xGa_{1-x}As$/GaAs heterojunction. The absorption was computed between the extended valence-band states and the quantum-confined states of the conduction band. The absorption edge is broad ($\sim$50 meV) and the onset is at approximately the band-gap energy. Since onset of the absorption for the excited subband states is at the band-gap energy, no structure is evident in the absorption profile that corresponds directly to the subband energy spacing. The modulation of the absorption was calculated corresponding to a change in n_s. The dominant modulation mechanism is the shift of the Burstein-Moss edge in the bottom subband. Consequently, $\Delta\alpha$ approximates the first derivative of α_0. Experimental ER data were found to qualitatively agree with the calculation.

This work was funded, in part, by the Office of Naval Research. We thank D. Broido and S. Kirchoefer for valuable assistance with the calculation.

[1]O. J. Glembocki, B. V. Shanabrook, N. Bottka, W. T. Beard, and J. Comas, Appl. Phys. Lett. **46**, 970 (1985).
[2]O. J. Glembocki, B. V. Shanabrook, N. Bottka, W. T. Beard, and J. Comas, SPIE Proc. **524**, 86 (1985).
[3]P. Parayanthal, H. Shen, F. H. Pollak, Micha Tomkiewicz, T. J. Drummond, and J. N. Schulman, Appl. Phys. Lett. **48**, 653 (1986).
[4]H. Shen, P. Parayanthal, Fred H. Pollak, O. J. Glembocki, B. V. Shanabrook, and W. T. Beard, Appl. Phys. Lett. **48**, 1261 (1986).
[5]B. V. Shanabrook, O. J. Glembocki, and W. T. Beard, Phys. Rev. B **35**, 2540 (1987).
[6]W. M. Theis, G. D. Sanders, C. E. Leak, K. K. Bajaj, and H. Morkoç, Phys. Rev. B **37**, 3042 (1988).
[7]Tang Yinsheng and Jiang Desheng, Chin. Phys. Lett. **4**, 283 (1987).
[8]D. E. Aspnes, in *Handbook on Semiconductors*, edited by T. E. Moss (North-Holland, New York, 1980), p. 109.
[9]R. A. Hopfel, J. Shah, A. C. Gossard, and W. Wiegmann, Appl. Phys. Lett. **47**, 163 (1985).
[10]O. Aina, M. Mattingly, F. Y. Juan, and P. K. Bhattacharya, Appl. Phys. Lett. **50**, 43 (1987).
[11]L. W. Molenkamp, G. W. 't Hooft, W. A. J. A. van der Poel, and C. T. Foxon, J. Phys. (Paris) Colloq. **48**, C5-127 (1987).
[12]Y. R. Yuan, K. Mohammed, M. A. A. Pudensi, and James L. Merz, Appl. Phys. Lett. **45**, 739 (1984).
[13]W. Ossau, E. Bangert, and G. Weimann, Solid State Commun. **64**, 711 (1987).
[14]C. B. Duke, Phys. Rev. **159**, 632 (1967).
[15]Tsuneya Ando, Alan B. Fowler, and Frank Stern, Rev. Mod. Phys. **54**, 437 (1982).
[16]Frank Stern and Sankar Das Sarma, Phys. Rev. B **30**, 840 (1984), and references therein.
[17]Max Born and Emil Wolf, *Principles of Optics* (Pergamon, New York, 1975).
[18]In the calculation, the 2D EG was assumed to arise from charge transfer from the doped $Al_xGa_{1-x}As$ layer. The electric field originating from the positive charge in the $Al_xGa_{1-x}As$ is screened from the GaAs depletion region by the 2D EG.
[19]N. Bottka, D. K. Gaskill, R. S. Sillmon, R. Henry, and R. Glosser, J. Electron. Mater. **17**, 161 (1988).